Second-order magnetoelectric susceptibility in the optical region: The case of boracite $Cu_3B_7O_{13}Br$

B. B. Krichevtsov and A. Yu. Zyuzin
A. F. Ioffe Physico-Technical Institute of Russian Academy of Sciences, 194021 St. Petersburg, Russia

H.-J. Weber
Physics Department, Dortmund University, 44221 Dortmund, Germany
(Received 21 May 2003; published 20 November 2003)

In the cubic phase of boracite $Cu_3B_7O_{13}Br$ (symmetry class T_d) the anisotropy and dispersion of nonreciprocal linear dichroism (ND) and nonreciprocal linear birefringence (NB) have been studied. The two magnetic-field-induced effects belong to the class of spatial dispersion phenomena. They have been observed near to the two strong absorption bands at the photon energies $E_{01}=1.5$ eV and $E_{02}=1.2$ eV. E_{01} and E_{02} are assigned to electronic transitions from the singlet ground state $^2B_2$ to states of the doublet ^2E. The analysis of dispersion of ND and NB is based on the crystal-field theory whereby spin-orbit coupling and Zeeman interaction have been included. An adequate description is obtainable only if the symmetry of the crystal field at Cu^{2+} ions is lower than tetragonal. Two mechanisms are discussed as the origin of symmetry reduction. At first, a structural disorder of halogen and/or metal ions in the boracite crystal lattice produces low-symmetry components of the crystal field and these components split the excited state ^2E. Second, symmetry is reduced by the dynamic Jahn-Teller effect.

DOI: 10.1103/PhysRevB.68.195114 PACS number(s): 71.70.Ch, 71.70.Ej, 78.20.−e

I. INTRODUCTION

Optical phenomena related to a nonlocal response of media to the action of electromagnetic waves are described by the dependence of the dielectric tensor ε_{ij} on the wave vector $\mathbf{k}$.[1,2] The linear in $\mathbf{k}$ components of the tensor ε_{ij} are nonzero in crystals and fluids possessing optical activity[3,4] and in some magnetically ordered crystals possessing spontaneous gyrotropic birefringence.[5–7] $\mathbf{k}$- linear terms of ε_{ij} can also be induced by external fields such as mechanical stresses, static electric and magnetic fields and their combinations.[8–12]

Magnetic-field-induced spatial dispersion (MISD) at optical frequencies has been investigated both theoretically and experimentally in noncentrosymmetric diamagnetic and paramagnetic semiconductors,[13–18] diamagnetic $LiIO_3$,[19] and in noncentrosymmetric fluids.[20,21]

Recently MISD has been observed in the paraelectric state of the crystalline boracite compounds $R_3B_7O_{13}X$ (abbreviated as RX in the following), where R^{2+} is a transition-metal ion and X^- is a halogen ion.[22–24] The crystal structure of boracites in the paraelectric state belongs to the noncentrosymmetric cubic class T_d. In this symmetry class optical activity is forbidden but in presence of the external magnetic field $\mathbf{B}$ the dielectric tensor $\varepsilon_{ij}(\omega,\mathbf{k},\mathbf{B})$ contains the terms $\gamma_{ijkl}B_k k_l$. Here γ_{ijkl} represents an axial i-tensor which contributes to the symmetric part of ε_{ij} and leads to the appearance of optical anisotropy. The Hermitian part of the tensor γ_{ijkl} describes the nonreciprocal linear birefringence (NB) and the anti-Hermitian part describes the nonreciprocal linear dichroism (ND). These optical phenomena can be observed most reliably for $\mathbf{B}\perp\mathbf{k}$, since in this geometry Faraday effect (FE) and magnetic circular dichroism (MCD) are absent.

The dependence of NB and ND on photon energy has been investigated in the past only in the boracite $Co_3B_7O_{13}I$ as far as dielectrics with paramagnetic ions are concerned. Electronic transitions between states of the Co^{2+} ion which show the configuration $3d^7$ have been studied.[22,24,25] A theoretical treatment of MISD optical phenomena in boracites has been carried out in Refs. 22 and 26. According to this theory MISD phenomena which are produced by local electronic transitions are related to the second-order magnetoelectric (ME) susceptibility and to the quadrupole mechanism. In Ref. 26 the dependence of NB on temperature, wavelengths, and azimuthal angles in the region of the transition $^4A_2(^4F)\rightarrow{}^4E(^4P)$ in CoI was described by use of the ME mechanism only. It manifests itself as the interference of electric dipole $\mathbf{d}_{ab}$ and magnetic dipole $\mathbf{m}_{ba}$ moments of optical transitions between the states a and b. The relevant matrix elements are of the type $\mathrm{Re}\{d_{ab}m_{ba}\}$. The nonzero value of an electric dipole matrix elements in this model is due to the noncentrosymmetric environment of the paramagnetic ion, i.e., it is determined by odd components of the crystal field. The study of spectral behavior of ND and NB makes it possible to evaluate transition matrix elements which are of different origin from those related to absorption and MCD. The latter phenomena are related to matrix elements of the type $\mathrm{Re}\{d_{ab}d_{ba}\}$ and $\mathrm{Im}\{d_{ab}d_{ba}\}$.

The goals of this work are the spectroscopic study of NB and ND near to absorption bands of the Cu^{2+} ion (electronic configuration $3d^9$) in $Cu_3B_7O_{13}Br$, the comparison of these phenomena with absorption and Faraday effect, and the consideration of second-order magnetoelectric susceptibility on the basis of the crystal-field theory. We show that the local crystal field of tetragonal symmetry at Cu^{2+} ions cannot explain the experimentally observed dispersion of these phenomena. An adequate description is obtained by taking into account low-symmetry components of the crystal field which split the degenerate orbital states ^2E of the Cu^{2+} ion. The reduction of crystal-field symmetry is explained by disorder of positions of metal and/or halogen ions in the boracite crystal lattice or by the dynamic Jahn-Teller effect. We also

point out the different influences of electron-phonon interaction on electric dipole (absorption, FE) and electric dipole-magnetic dipole (ND, NB) optical phenomena.

II. EXPERIMENT

The investigation of NB in $Cu_3B_7O_{13}Br$ single crystals has been carried out by means of the polarimetric method described in Refs. 17 and 18. A Al_2O_3:Ti laser operating in the spectral range $\Delta\lambda = 720–980$ nm, a helium-neon laser ($\lambda = 633$ nm), and a laser diode ($\lambda = 670$ nm) have been used as light sources. The magnetic field, angular, and spectral dependencies of the polarization plane rotation have been measured for light passing through a sample and then through a quarter wave plate. The direction of the magnetic field **B** (maximal magnitude up to ± 1.5 T) is perpendicular to the wave vector **k**. For investigating ND the quarter wave plate has been removed from the optical path. The measured quantity in this case is the rotation of linearly polarized light passing through a sample positioned in a perpendicular magnetic field. In this geometry the relation between the difference of absorption coefficients $\Delta\alpha[\mathrm{cm}^{-1}]$ induced by **B** for two orthogonal polarizations of light and the specific rotation φ[rad/cm] is $\varphi = \Delta\alpha/4$ if the angle between the polarization plane of the incident light wave and a principal axis of linear dichroism is equal to $\pi/4$.[27] Note that for the measurements of ND it is of special importance to avoid contributions of FE since both effects produce a rotation of the polarization direction of the light wave. The condition $\mathbf{B} \perp \mathbf{k}$ can be adjusted very accurately by reducing the constant part of the magnetic-field-induced rotation of polarization when the azimuth of the sample is changed.

In contrast to FE, the rotation due to ND strongly depends on the azimuth of the crystal, i.e., on the angle Θ between the direction of magnetic field and crystal axes. A phenomenological analysis shows that these angular variations are described by odd harmonics of Θ.[18] The anisotropy of rotation produced by ND depends also strongly on the angle between the polarization **E** of incident light and the direction of magnetic field **B**. We investigated the anisotropies Δn (NB) and $\Delta\alpha$ (ND) for the two geometries $\mathbf{E} \| \mathbf{B}$ and $\mathbf{E}45\mathbf{B}$.[17,18]

Because of the strong absorption of $Cu_3B_7O_{13}Br$ in the investigated spectral range it was necessary to use samples of different thicknesses d. In order to obtain optimal sensitivities the measurements of NB and FE at the wavelengths 633 nm and 670 nm have been carried out on samples with $d = 800\mu$m and in the spectral range $\Delta\lambda = 720–980$ nm on samples with $d = 100\mu$m and 52 μm. Sensitivity for the rotation of the polarization plane is about 5×10^{-5} rad. For measurements of FE, magnetic fields of the magnitude up to 0.1 T have been applied parallel to **k**.

Single crystals of $Cu_3B_7O_{13}Br$ have been grown by the method described in Ref. 28. Samples of different thicknesses have been cut along (110) and (100) planes and polished by diamond powders. Orientations of samples have been determined with an accuracy of about 1° by using x-ray methods. All measurements have been performed at the temperature $T = 294$ K.

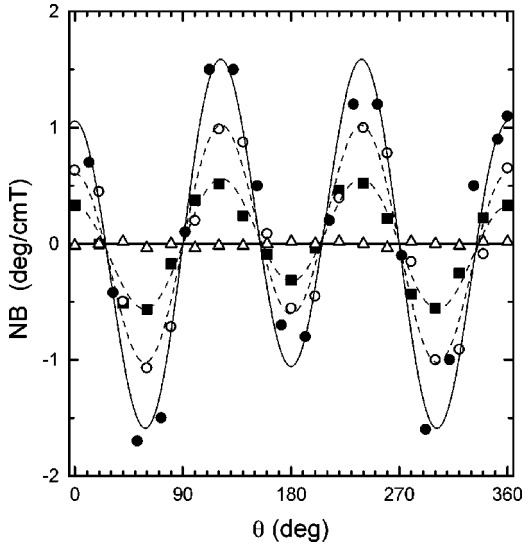

FIG. 1. Nonreciprocal linear birefringence NB of the boracite CuBr as a function of the azimuthal angle Θ. Measurements have been performed in the geometry $\mathbf{E} \| \mathbf{B}$ at the wavelengths $\lambda = 633$ nm (corresponding to 1.958 eV) (solid circles), $\lambda = 670$ nm (1.85 eV) (open circles), and $\lambda = 753$ nm (1.646 eV) (squares) in the crystallographic plane (110). Triangles represent data for the (100) plane and for $\lambda = 633$ nm. Lines correspond to fitting results.

III. RESULTS

Figure 1 shows the anisotropy of NB in CuBr boracite measured in the (110) plane at the wavelengths $\lambda = 633$ nm (equivalent to $E = 1.958$ eV), 670 nm (1.85 eV), and 754 nm (1.644 eV) in the geometry $\mathbf{E} \| \mathbf{B}$. It also shows results for the (001) plane and the wavelength $\lambda = 633$ nm. In the (110) plane NB is described by a linear combination of the odd harmonics $\cos\Theta$ and $\cos 3\Theta$, where Θ is the angle between the direction of **B** and the crystallographic axis [001]. The magnitude of NB increases with the wavelength from $\sim 0.6°/\mathrm{cm\,T}$ at $\lambda = 633$ nm to $\sim 1.5°/\mathrm{cm\,T}$ at $\lambda = 754$ nm but the character of anisotropy which is given by the ratio of the amplitudes of the first and the third harmonic of NB(Θ), does not change significantly. An analogous situation is observed in the geometry $\mathbf{E}45\mathbf{B}$. In this case NB(Θ) is described by $\sin\Theta$ and $\sin 3\Theta$ terms. In the (001) plane NB is absent. This result agrees with the symmetry analysis of the effect given in Refs. 17 and 18.

Figure 2 shows ND as a function of the azimuthal orientation of magnetic field in the (110) plane measured in geometry $\mathbf{E}45\mathbf{B}$ at the wavelengths 793 nm and 754 nm . ND is linear in the magnetic field **B**. The anisotropy of ND is described as in the case of NB by $\sin\Theta$ and $\sin 3\Theta$ terms. The magnitude of ND at $\lambda = 793$ nm and $\Theta = 90°$ is $\sim 6°/\mathrm{cmT}$ or $\Delta\alpha \sim 0.4\ \mathrm{cm}^{-1}\,\mathrm{T}^{-1}$. The strong anisotropy of ND and the absence of a significant background show that the measured rotations of the polarization plane are not affected by FE. From these observations we conclude that the residual misalignment of the magnetic field is less than about 1°.

Figure 3 shows the dispersion of NB, ND, and of the absorption coefficient α of the boracite CuBr. ND which is observable only in the absorption region is characterized by a

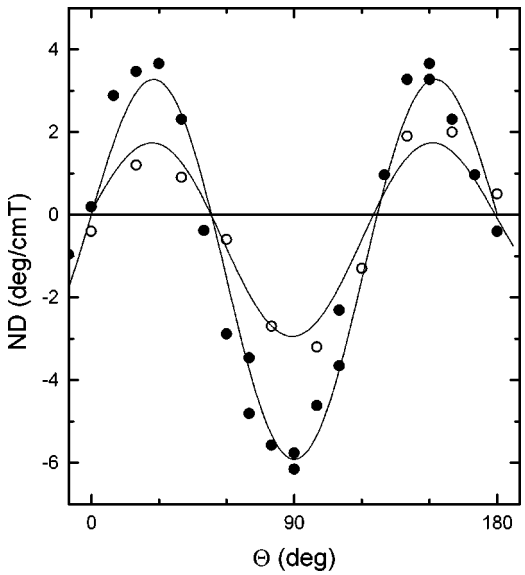

FIG. 2. ND of the boracite CuBr as a function of Θ in the geometry **E**45**B** in the plane (110) at λ = 754 nm (1.644 eV) (open circles) and λ = 793 nm (1.563 eV) (solid circles). Lines correspond to fitting results.

maximum at the photon energy $E = 1.5$ eV. It changes sign at $E = 1.35$ eV. In contrast to ND, NB is observed also in the transparent region. The magnitude of NB slowly increases with the decrease of photon energy and reaches maximal values in the region $E \sim 1.65$ eV. Then a further decrease of E leads to a decrease of NB. FE shows a maximum at $E = 1.65$ eV and the change of sign at $E = 1.5$ eV. Note the considerable difference in spectral variations of ND and FE. ND reaches the largest values near $E \sim 1.5$ eV at which the magnitude of FE is close to zero and changes its sign. Maximal values of FE are observed at the photon energy at which ND varies monotonically. This spectral behavior demonstrates that FE did not falsify the measurements of ND. The magnitudes of specific ND obtained for samples of different thicknesses ($d = 100\mu$m and 52μm) are practically the same in the spectral range 720–800 nm. This means that we can neglect reflection effects. We checked the independence of the magnitude of NB and ND on the intensity of the incident light and therefore we are able to exclude the action of nonlinear optical effects which can arise in a noncentrosymmetric crystal in applied magnetic field.

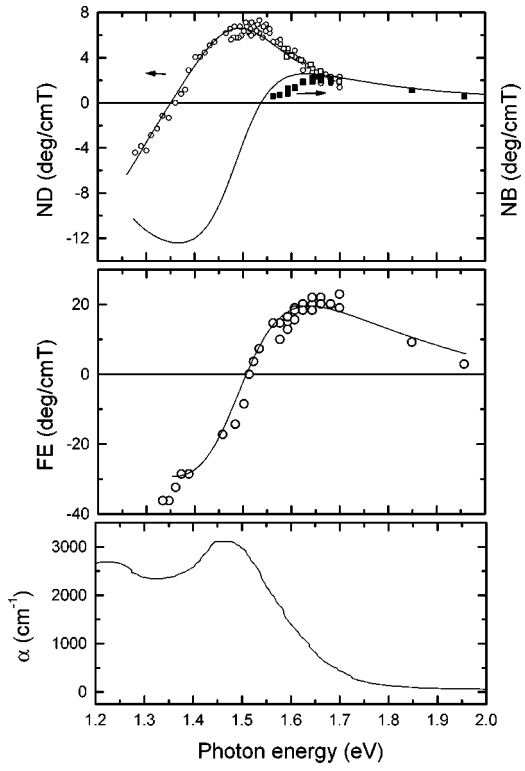

FIG. 3. Dispersion of ND, NB, FE, and of the absorption coefficient α (taken from Ref. 29) of the boracite CuBr. Lines for ND, NB, and FE have been calculated by use of a model with two Lorentz oscillators.

IV. THEORY AND DISCUSSION

Structural studies of the cubic phase (symmetry class T_d) of boracites have shown that the metal ions are placed in the center of octahedrons constructed by four oxygen ions and two halogen ions.[30,31] Symmetry class of the complex is D_{2d} and crystallographic site symmetry of the metal ion is S_4. The shift of oxygen ions of ~0.2 Å from the basal plane of the octahedron removes the inversion center and produces the odd crystal field $V^- = \alpha xyz$, (x,y,z are local axes of the complex, $x \| C_2', z \| S_4$) which mixes the wave functions of paramagnetic ions of opposite parity. Note that the possibility of quasistatic thermal distributions of halogen and/or metal ions on differently shifted positions has been discussed in the literature.[32,33] In this case the local symmetry of the crystal field at sites of the Cu^{2+} ion should be lower than tetragonal. Previous x-ray studies of boracites were not able to confirm or to disprove this suggestion but some arguments in favor of the absence of such distribution have been given.[30,31] Recent observation of two different metal-halogen distances and noncubic environment of halogen ions in the cubic phase of boracite $Fe_3B_7O_{13}I$ by means of extended x-ray-absorption fine structure (EXAFS) (Ref. 34) show nevertheless the reality of this possibility.

The nonfilled $3d$ electronic shell of the Cu^{2+} ion has nine electrons, i.e., one hole. The optical transitions are between states of the free ion ^2D term, which is split by the crystal field V_{cr}. Splitting of the ^2D term in cubic (O_h), tetragonal (D_{2d}), and low-symmetry crystal fields is shown schematically in Fig. 4. Optical transitions which are allowed both in electric- and magnetic dipole approximations are transitions from the ground state $^2B_2$ to the excited state ^2E. The transition to the state $^2B_1$ is forbidden in electric dipole approximation. Let us consider at first ND and NB for the transition $^2B_2 \rightarrow {}^2E$ assuming that the symmetry of the complex is D_{2d}.

Anisotropy of NB in different boracites (CoI, NiBr, CuBr) at the wavelength λ = 633 nm slightly depends on the type of the paramagnetic ion.[23] Such type of anisotropy is characterized by the definite relation $A = 2g$ between the two indepen-

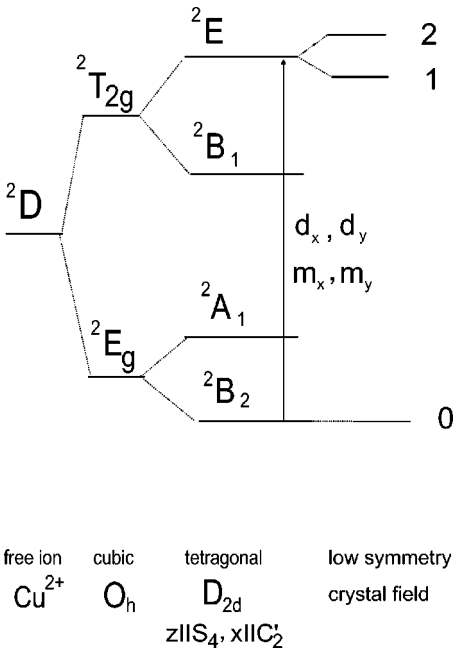

FIG. 4. Splitting of the ^2D state of Cu^{2+} ion in cubic, tetragonal, and low-symmetry crystal field.

dent components A and g of the tensor γ_{ijkl}. In the case of local transitions this relation has to be seen as a manifestation of the second-order magnetoelectric susceptibility in the optical region.[22] Figure 1 shows that the character of anisotropy of NB in the boracite CuBr does not depend significantly on the photon energy. This also shows the importance of the ME mechanism. A further argument for this conclusion stems from the similar anisotropy of NB in the transparent region (observed recently[23]) and of ND in the absorbing region (shown in Fig. 2) for the geometry **E**45**B**. The same type of ND anisotropy has been observed in the region of absorption bands of CoI boracite.[24] Therefore we consider only the ME mechanism in our calculations.

For almost filled $3d$ shell of Cu^{2+} ion it is convenient to use the hole representation. Wave functions of the states ^2E ($\eta_\pm$) and $^2B_2$ (v) in the local coordinate system x,y,z are

$$\eta_\pm = \sqrt{\frac{15}{8\pi}} \frac{z\left[x\exp\left(\pm\frac{i\pi}{4}\right) - y\exp\left(\mp\frac{i\pi}{4}\right)\right]}{r^2} R_{3d}(r), \quad (1)$$

$$v = -\sqrt{\frac{15}{4\pi}} \frac{xy}{r^2} R_{3d}(r), \quad (2)$$

where $R_{3d}(r)$ is the radial part of $3d$ wave function.

Electric and magnetic dipole transition momenta for transition $^2B_2 \rightarrow {}^2E$ in "closure approximation"[7] have the form

$$\langle \eta\pm|\mathbf{P}|0\rangle = p_0\left[\exp\left(\mp\frac{i\pi}{4}\right), -\exp\left(\pm\frac{i\pi}{4}\right), 0\right], \quad (3)$$

$$\langle \eta\pm|\mathbf{M}|0\rangle = \frac{i\mu}{\sqrt{2}}\left[\exp\left(\mp\frac{i\pi}{4}\right), \exp\left(\pm\frac{i\pi}{4}\right), 0\right], \quad (4)$$

where p_0 is a dipole element which in closure approximation is considered as a fitting parameter. μ is the Bohr magneton.

The spin-orbit coupling $H_{SO}=\Lambda \mathbf{S}\cdot\mathbf{L}$ and the Zeeman interaction $H_Z=\mu(\mathbf{L}+2\mathbf{S})\mathbf{B}$ give the change of energy difference between the excited and the ground states as

$$\langle \eta_\pm|H_{SO}|\eta_\pm\rangle - \langle v|H_{SO}|v\rangle = \pm\Lambda S^z, \quad (5)$$

$$\langle \eta_\pm|H_Z|\eta_\pm\rangle - \langle v|H_Z|v\rangle = \pm\mu B^z. \quad (6)$$

For the complex parameter A, which describes the contribution of the second-order magneto electric susceptibility to ND and NB, we have the following expression:[22]

$$A = K\sum_{a;b}\left\{\frac{d}{d\mathrm{B}_z}[\rho_a(\mathrm{B}_z)Z(E_{ab})\mathrm{Re}P^x_{ab}M^y_{ba}] + \curvearrowright\right\}, \quad (7)$$

where indices a and b denote the ground and excited states, $E_{ab}=E_b-E_a$, $Z(E_{ab})$ is the Lorentz form factor

$$Z(E_{ab}) = E_{ab}[E^2_{ab}-E^2+iE\Gamma]/E[(E^2_{ab}-E^2)^2+\Gamma^2E^2],$$

and $\curvearrowright$ means the cyclic permutation of x, y, z. $\rho_a(\mathrm{B}_z)$ is the density matrix. $K=32\hbar\cos 2f/e\Delta V$, where ΔV is the volume of the unit cell, and $f\approx 24°$. Substituting Eqs. (3)–(6) into Eq. (7) and averaging over spin variables, we obtain

$$A = \sqrt{2}p_0\mu^2 KC\frac{\partial[Z(E_{03})]}{\partial E_0}, \quad (8)$$

where $C=(1-\Lambda/2kT)$ (for Cu^{2+} ion $\Lambda=-850\ \mathrm{cm}^{-1}$). $E_{03}=E_3-E_0$, E_0 is the energy of the ground state $^2B_2$ and E_3 is the energy of excited state ^2E. The real part of A describes NB(E) and the imaginary one ND(E). Expression (8) predicts the S-type dispersion for ND(E) and the correspondence of NB(E) dispersion to the derivative $\partial\mathrm{ND}(E)/\partial E$.

The absorption spectrum of CuBr boracite between 0.8 eV and 2.0 eV consists of two wide bands with the resonance energies $E_{01}=1.5$ eV and $E_{02}=1.2$ eV and the bandwidths $\Gamma_{01}=0.2$ eV and $\Gamma_{02}=0.3$ eV at room temperature (Fig. 3). The large value of absorption in these bands of $\alpha \sim 3000\ \mathrm{cm}^{-1}$ indicates the electric dipole character of optical transitions (oscillator strength $\sim 10^{-3}$). Thus, the parity prohibition of these transitions is effectively removed by noncentrosymmetric crystal-field components and additionally by odd phonons.

The ND spectrum of CuBr boracite in the investigated spectral range can be described as the sum of the imaginary parts of two Lorentz oscillators. Resonance energies E_{0i} and damping parameters Γ_{0i} ($i=1,2$) of these oscillators are the same as in the absorption spectrum. The solid line in Fig. 3 shows the results of best fitting of ND with oscillators amplitudes as fitting parameters. The amplitudes of oscillators for bands at $E_{01}=1.5$ eV and $E_{02}=1.2$ eV have opposite signs and are of the same order of magnitude. Using the parameters of oscillators obtained from the ND spectrum it is possible to calculate the spectral dependence of NB related to these bands. Results of these calculations are presented in Fig. 3 by the solid line. Both the value and the spectral behavior of NB in the range $\Delta E=(1.5\text{–}2.0)$ eV are close to

experimental results. It shows that ND and NB obey the Kramers-Kronig relation and that the contribution to NB from transitions with higher energy $E>3$ eV is negligible. This is possible because the contributions to NB from different optical transitions may have different signs and compensate each other in the transparent region.

The absorption bands at $E_{01}=1.5$ eV and $E_{02}=1.2$ eV have been interpreted earlier as optical transitions between the states $^2B_2 \rightarrow {}^2E$ and $^2B_2 \rightarrow {}^2B_1$.[29] The energy difference of these transitions has been associated with the splitting of the $^2T_{2g}$ state in a tetragonal crystal field. Such an interpretation is reasonable but some new experimental facts require a revision, at least in the copper compound CuBr boracite:

(i) In both absorption bands E_{01} and E_{02} a very strong absorption ($\alpha \sim 3000$ cm^{-1}) appears in spite of the fact that the transition $^2B_2 \rightarrow {}^2B_1$ [wave function of $^2B_1$ state is $\zeta = \sqrt{15/16\pi}((x^2-y^2)/r^2)R_{3d}(r)$] is forbidden and $^2B_2 \rightarrow {}^2E$ is allowed in electric dipole approximation.

(ii) The bell-shape dispersion of ND and the *S*-type dispersion of NB observed for the band at $E_{01}=1.5$ eV does not correspond to that described by expression (8). Indeed in the case of *S*-type ND dispersion the maximum value of ND should be observed near $E=1.65$ eV but not at the transition resonance energy $E=1.5$ eV as observed in the experiment. Furthermore, NB should reach its maximum value at the resonance energy but in the experiment it goes to zero (see Fig. 3).

These contradictions can be removed if we assume that the symmetry of the crystal field at sites of the Cu^{+2} ion in the boracite crystal lattice is lower than tetragonal. This situation is possible if there is the distribution of the metal ions and/or halogen ions on several positions which are shifted relatively to those in the ideal crystal structure. In the presence of low-symmetry components of the crystal field the state ^2E is split and the main contribution to splitting is due to components of the crystal-field type $\delta V_{cr}=\beta(x^2-y^2)+\gamma xy$. In particular, the component γxy can arise as a consequence of Cu^{2+} shifting along *z* axes and both components, $\beta(x^2-y^2)$ and γxy may appear due to shifts of halogen ions along crystallographic axes of the [111] type.

Let us consider the spectral behavior of ND and NB for the case of a low-symmetry crystal field when the state ^2E is split into the states 1 and 2 by energy intervals $\Delta>\Gamma$ and $\Delta>\Lambda$ (Fig. 4). Removing degeneracy we obtain two states with wave functions

$$\Psi_1 = a\,\eta_+ + a^*\,\eta_-,$$

$$\Psi_2 = a\,\eta_+ - a^*\,\eta_-, \tag{9}$$

where $a=1/\sqrt{2}\exp(i\phi)$ and

$$\phi = \arctan\left(\frac{\int d\mathbf{r} \dfrac{z^2(x^2-y^2)}{r^4} V_{cr} R_d^2(\mathbf{r})}{2\int d\mathbf{r} \dfrac{z^2 xy}{r^4} V_{cr} R_d^2(\mathbf{r})} \right).$$

Electric and magnetic dipole transition matrix elements for transitions $0\rightarrow 1$ (transition energy E_{01}) and $0\rightarrow 2$ (transition energy E_{02}) are

$$\langle 1|\mathbf{P}|0\rangle = \sqrt{2}p_0\left[\cos\left(\phi+\frac{\pi}{4}\right), -\cos\left(\phi-\frac{\pi}{4}\right), 0\right],$$

$$\langle 2|\mathbf{P}|0\rangle = i\sqrt{2}p_0\left[-\sin\left(\phi+\frac{\pi}{4}\right), \sin\left(\phi-\frac{\pi}{4}\right), 0\right], \tag{10}$$

and

$$\langle 1|\mathbf{M}|0\rangle = \frac{i\mu}{2}\left[\cos\left(\phi+\frac{\pi}{4}\right), \cos\left(\phi-\frac{\pi}{4}\right), 0\right],$$

$$\langle 2|\mathbf{M}|0\rangle = \frac{i\mu}{2}\left[\sin\left(\phi+\frac{\pi}{4}\right), \sin\left(\phi-\frac{\pi}{4}\right), 0\right]. \tag{11}$$

In this case $\mathrm{Re}P_xM_y=\mathrm{Re}P_yM_x=0$. The inclusion of spin-orbit coupling and Zeeman interaction give the following corrections to matrix elements:

$$\delta\mathbf{P}_{01} = -\sqrt{2}i\frac{p_0}{\Delta}C\mathrm{B}_z\left[\sin\left(\phi+\frac{\pi}{4}\right), -\sin\left(\phi-\frac{\pi}{4}\right), 0\right], \tag{12}$$

$$\delta\mathbf{P}_{02} = \sqrt{2}\,\frac{p_0}{\Delta}C\mathrm{B}_z\left[\cos\left(\phi+\frac{\pi}{4}\right), -\cos\left(\phi-\frac{\pi}{4}\right), 0\right], \tag{13}$$

$$\delta\mathbf{M}_{01} = \frac{\mu}{\Delta}C\mathrm{B}_z\left[\sin\left(\phi+\frac{\pi}{4}\right), \sin\left(\phi-\frac{\pi}{4}\right), 0\right], \tag{14}$$

$$\delta\mathbf{M}_{02} = \frac{\mu}{\Delta}iC\mathrm{B}_z\left[\cos\left(\phi+\frac{\pi}{4}\right), \cos\left(\phi-\frac{\pi}{4}\right), 0\right]. \tag{15}$$

As a result we have

$$A = K\sum_{a=0;b=1,2}\frac{d}{d\mathrm{B}_z}[\rho_a(\mathrm{B}_z)Z(E_{ab})\mathrm{Re}P_{ab}^xM_{ba}^y]$$

$$= -\sqrt{2}\,\frac{p_0\mu^2}{\Delta}KC\{Z(E_{01})-Z(E_{02})\}. \tag{16}$$

We see that in crystal fields of low symmetry ND's for transitions 1 and 2 are described by a bell-shape dispersion with opposite signs. Dispersion of NB's for these transitions is *S* shaped and they are characterized by opposite signs which is in agreement with the experiment (Fig. 3).

Note that for the calculation of parameter *A* it is necessary to average the expression (7) over all possible complexes involving Cu^{2+} ions, taking into account that in different complexes the components of the crystal field may be different. In particular, components $\beta(x^2-y^2)$ and γxy have different signs in complexes which are transformed to each other by the symmetry operation S_4. The difference of the wave functions of such complexes is described by the phase ϕ. The change of sign of these crystal-field components,

which are responsible for the splitting of ^2E state, is equivalent to the change $\phi \rightarrow \phi + \pi$ in Eqs. (10)–(15). So, if in calculations of parameter A the terms involving $\sin\phi$ or $\cos\phi$ appear, they should be omitted. We can see that expression (16) does not contain such terms. The crystal-field components, which do not split ^2E state but shift the energy of ground and excited states, also may be different in different types of complexes. The influence of these components should manifest itself in additional broadening of absorption and ND bands, but not in the sign of ND.

Let us consider the different influences of symmetry reduction in the electric dipole type (absorption, FE) and the electric-magnetic dipole type (NB, ND) optical phenomena. The reduction of the crystal-field symmetry may be quasistatic, related to the disorder in distribution of metal or halogen ions in the crystal lattice, or dynamic due to the motion of ions around their equilibrium positions. In the case of centrosymmetric environment of the paramagnetic ion the electric dipole transitions between states of $3d$ shell of metal ion are allowed due to the electron-phonon interaction. Parity prohibition is violated by odd crystal-field components δV_{cr}^{-} which fluctuate in space and time. As a result the electric dipole moment $\delta \mathbf{d}_{ab}$ appears. The averaged value is $\langle \delta \mathbf{d}_{ab} \rangle = 0$, but $\langle \delta \mathbf{d}_{ab}^2 \rangle \neq 0$, which gives nonzero values of $\langle \mathrm{Re}(d_{ab}^i d_{ba}^j) \rangle$ and $\langle \mathrm{Im}(d_{ab}^i d_{ba}^j) \rangle$, i.e., absorption and FE. At the same time in such complexes second-order ME effect and MISD phenomena are forbidden because $\langle \delta d_{ab}^i m_{ba}^j \rangle = 0$. In the case of noncentrosymmetric environment the crystal field has the form: $V_{cr} = V_{cr}^{+} + V_{cr}^{-} + \delta V_{cr}^{+} + \delta V_{cr}^{-}$, where V_{cr}^{+} and V_{cr}^{-} are static even and static odd parts of the crystal field and δV_{cr}^{+} and δV_{cr}^{-} are fluctuating fields. Crystal-fields V_{cr}^{+} and δV_{cr}^{+} determine the energy of the electronic transition E_{ab} and fluctuations of E_{ab} due to changes of the crystal-field parameters D_q, D_s, and D_t. The odd crystal fields V_{cr}^{-} and δV_{cr}^{-} produce the electric dipole moment $\mathbf{d}_{ab}$ of transition and fluctuations $\delta \mathbf{d}_{ab}$, correspondingly. Because $\langle \delta \mathbf{d}_{ab} \rangle = 0$ the following equality is valid $\langle Z(E_{ab})(d_{ab}^i + \delta d_{ab}^i) m_{ba}^j \rangle = \langle Z(E_{ab}) d_{ab}^i m_{ba}^j \rangle$, i.e., the fluctuations δV_{cr}^{-} of the odd part of the crystal field do not contribute to ND and NB. We conclude that the appearance of new components of electric dipole momentum matrix elements due to dynamic deformations does not influence MISD phenomena in contrast to absorption and FE. If we assume that the absorption band at $E = 1.2$ eV corresponds to the transition $^2\mathrm{B}_2 \rightarrow {}^2\mathrm{B}_1$ and this transition is allowed in electric dipole approximation by electron-phonon interaction, we should not expect any ND for this band. But, experiment demonstrates the opposite behavior.

The quasistatic part of δV_{cr}^{+} does not provide principally new contributions to MISD, but this part makes it possible to explain the splitting of absorption bands of $Cu_3B_7O_{13}Br$ and the different signs of ND and NB observed in the experiment. In principal, the splitting of the absorption band $^2\mathrm{B}_2 \rightarrow {}^2E$ may be caused by the dynamic part of δV_{cr}^{+} due to the dynamic Jahn-Teller effect. In this case the description of ND and NB does not differ from the case of a quasistatic crystal field, at least in principle. The only difference is the method of averaging of Eq. (7) . Instead of averaging over different types of complexes we should average over shifts of ions taking into account the anisotropy of their motion.[31] Nevertheless, in the boracite CuBr the magnitude of absorption band splitting $\Delta E = 0.3$ eV does not change significantly in the ferroelectric phase below $T_c = 225$ K although metal and halogen ions are shifted statically from ideal positions. This correlates with the observation of two different metal-halogen distances in the wide temperature range including both the cubic and ferroelectric phase in the boracite FeI.[34]

In the boracite $Co_3B_7O_{13}I$ in the spectral region of the $^4A_2(^4F) \rightarrow {}^4E(^4P)$ transition ND shows the bell-type and NB the S type dispersion[22,24] but the reason for this behavior differs from that in the boracite CuBr.[26] In the boracite CoI this type of dispersion is related to spin-orbit mixing of the ground $^4A_2(^4F)$ state and the lowest $^4E(^4F)$ state that results in the appearance of new components of magnetic dipole matrix elements of the transition $^4A_2(^4F) \rightarrow {}^4E(^4P)$. In contrast to that in the case of the boracite CuBr the spin-orbital mixing of the ground state $^2\mathrm{B}_2$ and the nearest state $^2A_1$ [wave function of $^2A_1$ state is $u = \sqrt{5/16\pi}((3z^2 - r^2)/r^2) R_{3d}(r)$] does not modify electric and magnetic dipole matrix elements. Note that in contrast to the present result the spectra of ND in the boracite CoI do not show directly the big splitting of $^4E(^4P)$ state in low-symmetry crystal field.

V. CONCLUSION

We summarize the main results of the present paper as follows.

(i) In the cubic phase of the boracite $Cu_3B_7O_{13}Br$ the MISD optical phenomena, nonreciprocal linear birefringence, and nonreciprocal linear dichroism show the same type of anisotropy in a wide spectral range. The relation between the two parameters of the tensor γ_{ijkl} which describes the anisotropy of ND and NB shows that the effect is originated in a second-order magnetoelectric susceptibility for optical frequencies.

(ii) In the region of the absorption bands at $E_{01} = 1.5$ eV and $E_{02} = 1.2$ eV, ND and NB have opposite signs and show the bell-type and S-type dispersion. This result cannot be explained by a tetragonal crystal field acting at the sites of Cu^{2+} ions.

(iii) Contradictions between experimental results and theoretical description can be reconciled if the symmetry of the crystal field at sites of Cu^{2+} ions is lower than tetragonal. In this case the excited state of the relevant electronic transitions from the ground state $^2\mathrm{B}_2$ to ^2E is split by the low-symmetry components of the crystal field. The reduction of crystal field symmetry may be related to the disorder of positions of halogen or metal ions or to the dynamic Jahn-Teller effect for transition orbital singlet-orbital doublet.

(iv) Differences in the influence of electron-photon interaction on matrix elements of the type $\{d_{ab} d_{ba}\}$ (absorption, Faraday effects) and of the type $\{d_{ab} m_{ba}\}$ (nonreciprocal linear dichroism and birefringence) have been pointed out. These differences have been used to conclude from experimental results details of optical transitions and atomic positions which are difficult to obtain otherwise. Thus, second-

order magnetoelectric spectroscopy must be considered as an effective tool for the investigation of the electronic and crystallographic structure of a solid containing paramagnetic ions.

ACKNOWLEDGMENT

This work was supported by RFBR-DFG (Project No. 02-02-04003)

[1] L.D. Landau and E.M. Lifshitz, *Electrodynamics of Continuous Media* (Pergamon Press, New York, 1984).
[2] V.M. Agranovich and V.L. Ginzburg, *Spatial Dispersion in Crystal Optics and Theory of Excitons*, 2nd ed. (Springer-Verlag, Berlin, 1984).
[3] W. Kaminsky, Rep. Prog. Phys. **63**, 1575 (2000).
[4] E.U. Condon, Rev. Mod. Phys. **9**, 432 (1937).
[5] R.M. Hornreich and S. Shtrikmann, Phys. Rev. **171**, 1065 (1968).
[6] B.B. Krichevtsov, V.V. Pavlov, R.V. Pisarev, and V.N. Gridnev, Phys. Rev. Lett. **76**, 4628 (1996).
[7] M. Muto, Y. Tanabe, T. Iizuka-Sakano, and E. Hanamura, Phys. Rev. B **57**, 9586 (1998).
[8] B. Koopmans, P.V. Santos, and M. Cardona, Phys. Status Solidi B **205**, 419 (1998).
[9] H.J. Weber and S. Haussühl, Phys. Status Solidi B **65**, 633 (1974).
[10] D.L. Portigal, E.J. Burstein, Phys. Chem. Solids **32**, 603 (1971).
[11] H.-J. Weber, E.V. Balashova, and S.A. Kizhaev, J. Phys.: Condens. Matter **12**, 1485 (2000).
[12] T. Roth and G.L.J.A. Rikken, Phys. Rev. Lett. **85**, 4478 (2000).
[13] E.F. Gross, B.P. Zacharchenya, and O.V. Konstantinov, Fiz. Tverd. Tela (Leningrad) **3**, 305 (1961) [Sov. Phys. Solid State **3**, 221 (1961).
[14] V.P. Kochereshko, G.V. Michailov, and G.V. Uraltsev, Fiz. Tverd. Tela (Leningrad) **25**, 769 (1983) [Sov. Phys. Solid State **25**, 439 (1983)].
[15] E.L. Ivchenko, V.P. Kochereshko, G.V. Michailov, and I.N. Uraltsev, Phys. Status Solidi B **121**, 221 (1984).
[16] O.V. Gogolin, V.A. Tsvetkov, and E.G. Tsitsichvili, Zh. Eksp. Teor. Fiz. **60**, 1038 (1984) [Sov. Phys. JETP **60**, 593 (1984)].
[17] B.B. Krichevtsov, R.V. Pisarev, A.A. Rzhevsky, V.N. Gridnev, H.-J. Weber, Phys. Rev. B **57**, 14 611 (1998).
[18] B.B. Krichevtsov, R.V. Pisarev, A.A. Rzhevsky, V.N. Gridnev, and H.-J. Weber, Zh. Éksp. Teor. Fiz. **114**, 1098 (1998) [JETP **87**, 553 (1998)].
[19] V.A. Markelov, M.A. Novikov, and A.A. Turkin, Pis'ma Zh. Exp. Theor. Fiz. **25**, 404 (1977) [JETP Lett. **25**, 378 (1977)].
[20] N.B. Baranova, B.Ya. Zel'dovich, Mol. Phys. **38**, 1085 (1979).
[21] P. Kleindienst and G.H. Wagnière, Chem. Phys. Lett. **288**, 89 (1998).
[22] B.B. Krichevtsov, A.A. Rzhevskii, and H.-J. Weber, Phys. Rev. B **61**, 10084 (2000).
[23] B.B. Krichevtsov, Fiz. Tverd. Tela (St. Petersburg) **43**, 75 (2001) [Phys. Solid State **43**, 76 (2001)].
[24] B.B. Krichevtsov, JETP Lett. **74**, 159 (2001).
[25] B.B. Krichevtsov, Ferroelectrics **279**, 111 (2002).
[26] A.Yu. Zyuzin and B.B. Krichevtsov, Phys. Rev. B **65**, 045103 (2001).
[27] A.K. Zvezdin and V.A. Kotov, *Modern Magnetooptics and Magnetooptical Materials* (Institute of Physics, Bristol, 1997).
[28] H. Schmid, J. Phys. Chem. Solids **26**, 973 (1965).
[29] N.N. Nesterova, Ph.D. thesis, A. F. Ioffe Physico-Technical Institute of RAS, 1974.
[30] R.J. Nelms, J. Phys. C **7**, 3840 (1974)
[31] R.J. Nelms and W.J. Hay, J. Phys. C **14**, 5247 (1981).
[32] H. Schmid, Phys. Status Solidi A **37**, 209 (1970).
[33] E. Asher, J. Phys. Soc. Jpn., Suppl. **28**, 7 (1970).
[34] T.I. Nedoseykina, V.A. Shuvaeva, I.V. Pirog, A.T. Shuvaev, K. Yagi, and Y. Azuma, and H. Terauchi, *Book of Abstracts International Symposium on Ferroelectricity RCPJSF-7* (A. F. Ioffe Physico-Technical Institute of RAS, St. Petersburg, 2002), p. 91.